PHYSICAL REVIEW B **91**, 241117(R) (2015)

Solving the fermion sign problem in quantum Monte Carlo simulations by Majorana representation

Zi-Xiang Li,[1] Yi-Fan Jiang,[1,2] and Hong Yao[1,3,*]

[1]*Institute for Advanced Study, Tsinghua University, Beijing 100084, China*

[2]*Department of Physics, Stanford University, Stanford, California 94305, USA*

[3]*Collaborative Innovation Center of Quantum Matter, Beijing 100084, China*

(Received 27 August 2014; revised manuscript received 13 October 2014; published 30 June 2015)

We discover a quantum Monte Carlo (QMC) method to solve the fermion sign problem in interacting fermion models by employing a Majorana representation of complex fermions. We call it the "Majorana QMC" (MQMC). MQMC simulations can be performed efficiently both at finite and zero temperatures. Especially, MQMC is fermion sign free in simulating a class of *spinless* fermion models on bipartite lattices at half filling and with an arbitrary range of (unfrustrated) interactions. Moreover, we find a class of $SU(N)$ fermionic models with *odd* N, which are sign free in MQMC but whose sign problem cannot be in solved in other QMC methods, such as continuous-time QMC. To the best of our knowledge, MQMC is the first auxiliary field QMC method to solve the fermion sign problem in spinless (more generally, an odd number of species) fermion models. We conjecture that MQMC could be applied to solve the fermion sign problem in more generic fermionic models.

DOI: 10.1103/PhysRevB.91.241117 PACS number(s): 05.30.Fk, 02.70.Ss, 71.27.+a

Introduction. Interacting fermionic quantum systems with strong correlations and/or topological properties have attracted increasing attention [1,2]. Nonetheless, in two and higher spatial dimensions, strongly interacting quantum systems are generically beyond the reach of analytical methods in the sense of solving those quantum models in an unbiased way. As an intrinsically unbiased numerical method, the quantum Monte Carlo (QMC) simulation plays a key role in understanding the physics of strongly correlated many-body systems [3–7]. Unfortunately, in simulating fermionic many-body systems, QMC often encounters the notorious fermion minus-sign problem [8,9], which arises as a consequence of Fermi statistics [10]. Undoubtedly, generic solutions of fermion sign problems would lead to a great leap forward in understanding correlated electronic systems [9].

Many QMC algorithms are based on converting an interacting fermion model into a problem of free fermions interacting with background auxiliary classical fields; the Boltzmann weight is the determinant of the free fermion matrix which is a function of auxiliary fields and which can be positive, negative, or even complex. In such determinant QMC (DQMC), when the determinants are rendered to be positive definite, we say a solution to the fermion sign problem is found. For spinful electrons, the conventional strategy of solving the fermion sign problem is to find a symmetric treatment of both spin components of electrons such that the Boltzmann weight can be written as the product of two real determinants with the same sign and is then positive definite [11–16]. For spinless or spin-polarized fermion models, it is usually much more difficult to solve the fermion sign problem because the Boltzmann weight contains only a single determinant and the usual strategy used for even species of fermions cannot be directly applied here.

In this Rapid Communication, based on the Majorana representation of fermions, we propose an auxiliary field QMC approach to solve the fermion sign problem in spinless fermion models. We observe that each complex fermion can be represented as two Majorana fermions. Consequently, we can express spinless fermion Hamiltonians in a Majorana representation and then perform Hubbard-Stratonovich (HS) transformations to decouple interactions by introducing background auxiliary fields. Under certain conditions, such as particle-hole symmetry, we can find a symmetric treatment of two species of Majorana fermions, namely, the free Majorana fermion Hamiltonian obtained after HS transformations is a sum of two symmetric parts, each involving only one species of Majorana fermions, such that the Boltzmann weight is a product of two identical real quantities and is then positive definite. This is the basic idea of the Majorana approach to solve the fermion sign problem in spinless or spin-polarized fermion models which we call the "Majorana QMC" (MQMC). Note that the MQMC approach proposed here is qualitatively different from the meron-cluster method [17,18] and fermion bag method [19,20] developed previously, all of which are based on the continuous-time QMC (CTQMC) [20–23]. MQMC is a QMC approach based on auxiliary fields to solve the fermion sign problem in a class of spinless (more generally, an odd number of species) fermion models. Moreover, MQMC has an important advantage: It is much more efficient than continuous-time QMC in simulating models at low and zero temperatures; the computation-time cost in MQMC scales as $\beta \equiv 1/T$ while it scales as β^3 in continuous-time QMC [20] (see also more recent developments discussed in Ref. [24]).

As an application of the sign-free MQMC algorithm, we have used it to study the charge density wave (CDW) quantum phase transition of the spinless fermion model with repulsive density interactions on the honeycomb lattice with a much larger system size ($2L^2$ sites with L up to 24) than previous studies, and obtained quantum critical exponents which are in reasonable agreement with renormalization group (RG) calculations [25]. We also show that MQMC can solve the fermion sign problem in a class of $SU(N = \text{odd})$ models which are beyond the capability of other QMC methods, such as the continuous-time QMC.

Majorana quantum Monte Carlo. To explicitly illustrate how MQMC could solve the fermion sign problem in a class of spinless fermion models, we consider the following general

*yaohong@tsinghua.edu.cn

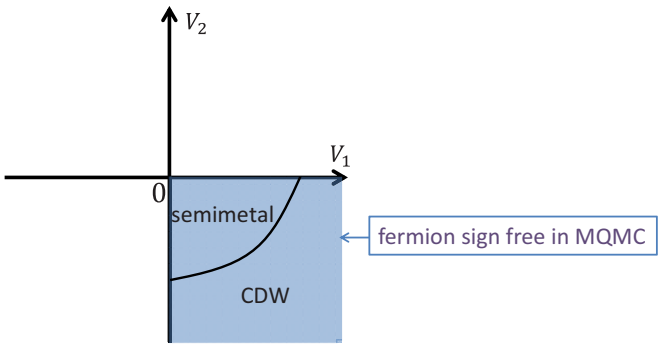

FIG. 1. (Color online) The schematic quantum phase diagram of the t-V_1-V_2 spinless fermion model on the honeycomb lattice in the region of $V_1 > 0$ and $V_2 < 0$. In this region, MQMC simulations at zero and finite temperatures can be performed efficiently without a fermion sign problem.

Hamiltonian of spinless fermions,

$$H = H_0 + H_{\text{int}}, \tag{1}$$

$$H_0 = -\sum_{ij}[t_{ij}c_i^\dagger c_j + \text{H.c.}], \tag{2}$$

$$H_{\text{int}} = \sum_{ij} V_{ij}(n_i - 1/2)(n_j - 1/2), \tag{3}$$

where $c_i^\dagger$ creates a fermion on site i, t_{ij} represents the hopping integral, and V_{ij} labels the density interaction. As we shall show below, the MQMC is fermion sign free when the Hamiltonian in Eq. (1) satisfies the following two conditions: (1) $t_{ij} \neq 0$ *only* when i, j belong to different sublattices; (2) $V_{ij} > 0$ when i, j belong to different sublattices, and $V_{ij} < 0$ when i, j belong to the same sublattices. With the first condition, it is clear that the model is invariant under particle-hole transformations, $c_i \to (-1)^i c_i^\dagger$, where $(-1)^i$ has opposite signs for different sublattices and then describes fermions at half filling. The lattice in question can be any bipartite lattice, such as honeycomb and square lattices in two dimensions (2D) as well as cubic and diamond lattices in three dimensions (3D). For simplicity, we hereafter consider the model with only nearest-neighbor (NN) hopping t, NN repulsive interaction V_1, and next-nearest-neighbor (NNN) attractive interactions V_2, which we call the t-V_1-V_2 model on the honeycomb lattice (generalizing the MQMC method to models with longer-range hopping and interactions will be straightforward). As shown in Fig. 1, MQMC is fermion sign free in the region where the quantum phase transition between the Dirac semimetal and charge density wave (CDW) phases occurs [22]. [It is interesting to note that the t-V_1-V_2 spinless fermion model on the honeycomb lattice features very interesting phases, including quantum anomalous Hall (QAH) phases [26] and pair density wave (PDW) phases [27].]

In statistical physics, a key quantity is the partition function. QMC methods are designed to simulate partition functions in a statistical fashion. For the t-V_1-V_2 model, the partition function after Trotter decomposition is given by

$$Z = \text{Tr}[e^{-\beta H}] \simeq \text{Tr}\left[\prod_{n=1}^{N_\tau} e^{-H_0(n)\Delta\tau} e^{-H_{\text{int}}(n)\Delta\tau}\right], \tag{4}$$

where $n = 1, \ldots, N_\tau$ labels the discrete imaginary time, $\Delta\tau N_\tau = \beta$, and the approximation is good for small $\Delta\tau$ or large N_τ. HS transformations can be applied to decouple fermion interactions into noninteracting terms interacting with background auxiliary fields. The usual HS decoupling in density channels normally results in a minus sign problem in QMC because the Boltzmann weight is a single determinant. However, we observe that the Hamiltonian can be rewritten in terms of Majorana fermions and there are two species of Majorana fermions. In the Majorana representation, complex fermion operators are given by

$$c_i = \tfrac{1}{2}(\gamma_i^1 + i\gamma_i^2), \quad c_i^\dagger = \tfrac{1}{2}(\gamma_i^1 - i\gamma_i^2), \tag{5}$$

which enable us to rewrite the Hamiltonian as follows:

$$H_0 = \sum_{\langle ij\rangle} \frac{it}{2}(\gamma_i^1\gamma_j^1 + \gamma_i^2\gamma_j^2),$$

$$H_{\text{int}} = -\frac{V_1}{4}\sum_{\langle ij\rangle}(i\gamma_i^1\gamma_j^1)(i\gamma_i^2\gamma_j^2) - \frac{V_2}{4}\sum_{\langle\langle ij\rangle\rangle}(i\gamma_i^1\gamma_j^1)(i\gamma_i^2\gamma_j^2),$$

where gauge transformations $c_i \to ic_i$ for i in only one sublattice were implicitly made so that H_0 can be written symmetrically in the two components of the Majorana fermions. Now, it is clear that we should perform HS transformations in Majorana hopping channels instead of density channels as is done in the usual QMC methods. Explicitly, HS transformations for interactions in H_{int} in MQMC are given by

$$e^{\frac{V_1\Delta\tau}{4}(i\gamma_i^1\gamma_j^1)(i\gamma_i^2\gamma_j^2)} = \frac{1}{2}\sum_{\sigma_{ij}=\pm1} e^{\frac{1}{2}\lambda_1\sigma_{ij}(i\gamma_i^1\gamma_j^1 + i\gamma_i^2\gamma_j^2) - \frac{V_1\Delta\tau}{4}}, \tag{6}$$

$$e^{\frac{V_2\Delta\tau}{4}(i\gamma_i^1\gamma_j^1)(i\gamma_i^2\gamma_j^2)} = \frac{1}{2}\sum_{\sigma_{ij}=\pm1} e^{\frac{1}{2}\lambda_2\sigma_{ij}(i\gamma_i^1\gamma_j^1 - i\gamma_i^2\gamma_j^2) + \frac{V_2\Delta\tau}{4}}, \tag{7}$$

where λ_1 and λ_2 are constants determined through $\cosh\lambda_1 = e^{\frac{V_1\Delta\tau}{2}}$ and $\cosh\lambda_2 = e^{\frac{-V_2\Delta\tau}{2}}$, respectively. Note that in Eq. (7) the signs of γ^1 hopping terms are opposite to γ^2 hopping terms in the HS decompositions of the NNN interaction because $V_2 < 0$. The same signs are obtained for the decoupling of NN interactions in Eq. (6) because $V_1 > 0$. It is now clear that the free fermion Hamiltonian after the HS transformations is a sum of two parts, each of which involves only one component of Majorana fermions. This makes MQMC simulations sign problem free because the Boltzmann weight can be positive definite, which we shall show below.

Note that auxiliary fields $\sigma_{ij}(n)$ should be introduced independently for each discrete imaginary time n. As a result, the partition function is a sum over the Boltzmann weight, which is a function of auxiliary field configurations in space-time, as given by

$$Z = \sum_{\{\sigma\}} W(\{\sigma\}). \tag{8}$$

Up to an unimportant constant, the Boltzmann weight $W(\{\sigma\})$ is given by

$$W(\{\sigma\}) = \text{Tr}\left[\prod_{n=1}^{N_\tau} e^{\sum_{a=1}^{2}\frac{1}{4}\tilde{\gamma}^a h^a(n)\gamma^a}\right], \tag{9}$$

where $\widetilde{\gamma}^a$ represents the transpose of γ^a and $h^a(n)$ is a $N \times N$ matrix ($N =$ the number of lattice sites) given by

$$h^a_{ij}(n) = i[t\Delta\tau\delta_{\langle ij\rangle} + \lambda_1\sigma_{ij}(n)\delta_{\langle ij\rangle} \pm \lambda_2\sigma_{ij}(n)\delta_{\langle\langle ij\rangle\rangle}], \quad (10)$$

where $\delta_{\langle ij\rangle} = \pm 1$ if ij are NN sites and 0 otherwise; similarly, $\delta_{\langle\langle ij\rangle\rangle} = \pm 1$ only if ij are NNN sites. Now, we can trace out the Majorana fermions since they are free, as shown in the Supplemental Material [28]. Because the two components of the Majorana fermions are decoupled, tracing out Majorana fermions can be done independently and the Boltzmann weight is a product of two factors,

$$W(\{\sigma\}) = W_1(\{\sigma\})W_2(\{\sigma\}),$$

where

$$W_a(\{\sigma\}) = \left\{\det\left[\mathbb{I} + \prod_{n=1}^{N_\tau} e^{h^a(n)}\right]\right\}^{\frac{1}{2}}. \quad (11)$$

Note that there is sign ambiguity when taking a square root above, similar to the case of a Pfaffian as a square root of determinants.

Fermion sign free. Now we prove that the Boltzmann weight is positive definite by showing that $W_1(\{\sigma\}) = W_2^*(\{\sigma\})$. A key observation is that the Hamiltonian $\hat{h}^1(n) \equiv \widetilde{\gamma}^1 h^1(n)\gamma^1$ of Majorana fermions γ^1 can be mapped to a Hamiltonian identical to $\hat{h}^2(n) \equiv \widetilde{\gamma}^2 h^2(n)\gamma^2$ by the following time-reversal transformation $\Theta = TK$, where K is the complex conjugation and T is given as below:

$$T : \gamma_i^1 \to (-1)^i \gamma_i^2, \quad (12)$$

Namely, $\widetilde{\gamma}^1 h^1(n)\gamma^1 \to \widetilde{\gamma}^2 h^2(n)\gamma^2$ under time reversal transformation Θ. Because the time-reversal transformation complex conjugates the results of tracing out Majorana fermions, we obtain

$$W_1(\{\sigma\}) = W_2^*(\{\sigma\}), \quad (13)$$

which renders the Boltzmann weight $W(\{\sigma\}) = W_1(\{\sigma\})W_2(\{\sigma\}) \geqslant 0$ for any auxiliary field configuration $\{\sigma\}$. Explicitly, it is

$$W(\{\sigma\}) = \left|\det\left[\mathbb{I} + \prod_{n=1}^{N_\tau} e^{h^a(n)}\right]\right|, \quad (14)$$

where $a = 1$ or 2, which gives rise to the same result. This proves that the MQMC algorithm can solve the fermion sign problem in such a class of models consisting of spinless fermions. It is the central result of this Rapid Communication.

Projector MQMC. The MQMC algorithm above simulates the finite-temperature partition function in the grand canonical ensemble by computing the trace shown in Eq. (9). If one is interested in ground state properties, it is advantageous to use the projector algorithm to carry out QMC [29–31] since the projector QMC is often more efficient than the finite-temperature QMC. The expectation value of an operator O in the ground state is given by

$$\frac{\langle\psi_0|\, O\, |\psi_0\rangle}{\langle\psi_0\mid\psi_0\rangle} = \lim_{\theta\to\infty} \frac{\langle\psi_T|\, e^{-\theta H} O e^{-\theta H}\, |\psi_T\rangle}{\langle\psi_T|\, e^{-2\theta H}\, |\psi_T\rangle}, \quad (15)$$

where $|\psi_0\rangle$ is the ground state and $|\psi_T\rangle$ is a trial wave function which we assume has a finite overlap with the true ground state. Here, $Z_T \equiv \langle\psi_T|e^{-2\theta H}|\psi_T\rangle$ plays the role of usual partition functions and needs to be expressed as a sum of Boltzmann weights. In practice, a Slater-determinant wave function describing noninteracting fermions is often chosen as the trial wave function in the projector QMC,

$$|\psi_T\rangle = \prod_{\alpha=1}^{N_f} (c^\dagger P)_\alpha |0\rangle, \quad (16)$$

where P is an $N \times N_f$ matrix (N_f labels the number of fermions in question). Usually, $|\psi_T\rangle$ is an eigenvector of the noninteracting part of the Hamiltonian in question, namely, H_0 in Eq. (1). In a Majorana representation of fermions, γ^1 and γ^2 Majorana fermions are decoupled in H_0; consequently, $|\psi_T\rangle = |\psi_T^1\rangle \otimes |\psi_T^2\rangle$. By introducing similar HS transformations and auxiliary fields $\{\sigma\}$ as above, the "partition function" is obtained as a sum of the Boltzmann weight $W(\{\sigma\})$ over auxiliary field configurations: $Z_T = \sum_{\{\sigma\}} W(\{\sigma\})$. Since γ^1 and γ^2 Majorana fermions are decoupled after the HS transformation, we again obtain $W(\{\sigma\}) = W_1(\{\sigma\})W_2(\{\sigma\})$, where

$$W_a(\{\sigma\}) = \left\langle\psi_T^a\right| \left[\prod_{n=1}^{N_\tau} e^{\frac{1}{4}\widetilde{\gamma}^a h^a(n)\gamma^a}\right] \left|\psi_T^a\right\rangle. \quad (17)$$

Similarly, $W_1(\{\sigma\}) = W_2^*(\{\sigma\})$ because of the time reversal symmetry Θ. As shown in the Supplemental Material [28], the Boltzmann weight is given by

$$W(\{\sigma\}) = \left|\det\left\{P_a^\dagger \left[\prod_{n=1}^{N_\tau} e^{h^a(n)}\right] P_a\right\}\right|, \quad (18)$$

where $a = 1$ or 2 and P_a is the projection matrix constructed from $|\psi_T^a\rangle$. Consequently, the projector MQMC is also free from the fermion sign problem for a class of spinless fermion models.

Physical observables in MQMC. One important advantage of auxiliary field QMC algorithms is that physical observables can be obtained conveniently. For instance, time- and space-dependent Green's functions can be computed directly in the DQMC algorithm. We show below that both at finite and zero temperature the computation of physical observables in MQMC is similarly convenient as that in the DQMC algorithm.

In QMC, physical observables can be related to a single-particle Green's function, $G_{ij} = \langle c_i^\dagger c_j\rangle$, where the average is done stochastically over auxiliary field configurations. In the Majorana representation, it is given by

$$\langle c_i^\dagger c_j\rangle = \tfrac{1}{4}\left(\left\langle\gamma_i^1\gamma_j^1\right\rangle + \left\langle\gamma_i^2\gamma_j^2\right\rangle\right), \quad (19)$$

where we used the results of $\langle\gamma_i^1\gamma_j^2\rangle = 0$, which is a consequence of the decoupling of the two species of Majorana fermions after the HS transformation. To obtain the Green's functions, we only need to compute $\langle\gamma_i^1\gamma_j^1\rangle$ and $\langle\gamma_i^2\gamma_j^2\rangle$. Because the two species of Majorana fermions are related by the time reversal symmetry Θ, we obtain $W_1(\{\sigma\}) = W_2^*(\{\sigma\})$. It is straightforward to evaluate the equal-time Majorana

Green's function $\langle \gamma_i^a \gamma_j^a \rangle$ in the finite-temperature MQMC,

$$G_{ij}^a = \sum_{\{\sigma\}} W(\{\sigma\}) \langle \gamma_i^a \gamma_j^a \rangle_\sigma = \frac{1}{2} \sum_{\{\sigma\}} W(\{\sigma\}) \left[\mathbb{I} + \prod_{n=N_\tau}^{1} e^{-h^a(n)} \right]_{ji}^{-1}, \quad (20)$$

where the factor 1/2 above comes from the nature of the Majorana fermions. Employing Wick's theorem for each configuration $\{\sigma\}$, higher-order correlation functions, including density-density and pair-pair correlations, can be obtained from single-particle Green's functions. For instance, the equal-time density-density correlations are given by $\langle (c_i^\dagger c_i - \frac{1}{2})(c_j^\dagger c_j - \frac{1}{2}) \rangle_\sigma = \frac{1}{4} \langle \gamma_i^1 \gamma_j^1 \rangle_\sigma \langle \gamma_i^2 \gamma_j^2 \rangle_\sigma$.

It is increasingly realized that quantum entanglement could play a key role in understanding quantum many-body systems [32–36]. Quantum entanglement is partially characterized by entanglement entropy, including the von Neumann entropy $S_{vN} = -\mathrm{Tr}[\rho_A \log \rho_A]$ and the Renyi entropy $S_n = -\frac{1}{n-1} \log[\mathrm{Tr}(\rho_A^n)]$, where ρ_A is the reduced density matrix of subregion A. Even though it is still challenging for auxiliary field QMC algorithms to evaluate the von Neumann entropy, it was shown recently that DQMC can provide an efficient way to evaluate the Renyi entropy by simulating the reduced density matrix ρ_A expressed in terms of the Green's function [37–38]. Because MQMC is able to compute Green's functions efficiently, the Renyi entropy can be calculated accurately in the MQMC algorithm as long as it is fermion sign free.

Numerical results. We performed highly accurate projector MQMC simulations to study the t-V_1-V_2 model on the honeycomb lattice at zero temperature. For simplicity, we set $t = 1$, $V_2 = 0$, and then vary V_1 to find the critical value of V_1, above which the system develops a finite CDW ordering at zero temperature. To measure the CDW order parameter Δ_{CDW}, we calculate the CDW structure factor at a finite lattice size,

$$M_2 = \sum_{ij} \frac{\eta_i \eta_j}{N^2} \left\langle \left(n_i - \frac{1}{2} \right) \left(n_j - \frac{1}{2} \right) \right\rangle, \quad (21)$$

where $\eta_i = +1(-1)$ on the $A(B)$ sublattice and $N = 2 \times L \times L$ is the total number of sites. It is obvious that $\lim_{L\to\infty} M_2 = \Delta_{\mathrm{CDW}}^2$. The simulations are done for lattices up to $L = 21$, which is substantially larger than the one in Ref. [22], indicating that our MQMC algorithm is quite efficient. As shown in Fig. 2(a), we obtain Δ_{CDW}^2 through finite-size scaling of the measured M_2 on lattices of $L = 9,12,15,18,21$. For instance, $\Delta_{\mathrm{CDW}} \approx 0.17 \pm 0.01$ at $V_1 = 1.42$. It is clear that the critical value of V_1 separating the semimetal and CDW phases is between 1.34 and 1.38. To obtain the critical value of V_1 more accurately, we calculate the Binder ratio defined as $B = \frac{M_4}{M_2^2}$ for various V_1 and L, where $M_4 = \sum_{ijkl} \frac{\eta_i \eta_j \eta_k \eta_l}{N^4} \langle (n_i - \frac{1}{2})(n_j - \frac{1}{2})(n_k - \frac{1}{2})(n_l - \frac{1}{2}) \rangle$. At the putative critical point, the Binder ratios for different L should cross. As shown in Fig. 2(b), the Binder ratios for $L = 12,15,18,21$ indeed cross nearly the same point when

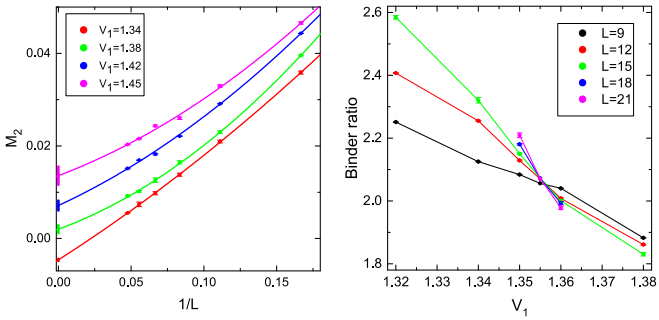

FIG. 2. (Color online) (a) Finite-size scaling of the CDW structure factor M_2 obtained in the projector (zero-temperature) MQMC simulations for various V_1 and $L = 9,12,15,18,21$. It is clear that the phase transition between the semimetal and the CDW phase occurs when V_1 is between 1.34 and 1.38. The error bars for measured quantities are show explicitly and they are negligibly small. (b) The Binder ratios $B \equiv M^4/M_2^2$ for various V_1, including $V_1 = 1.355$, and various $L = 9$–21, are plotted. From crossing of the Binder ratios, we conclude that the critical value of V_1 for the CDW transition is $V_{1c} = 1.355 \pm 0.001$.

$V_1 = 1.355$. Consequently, we conclude that the critical value $V_{1c} = 1.355 \pm 0.001$.

The critical exponents and universality class at the phase transition [39,40] have been analyzed through even larger-scale MQMC simulations by us [25]. Because the CPU time cost scales linearly with β, we were able to perform the MQMC simulations on a much larger system size ($L_{\max} = 24$) [25] than the one studied by CTQMC ($L_{\max} = 15$ there) [22]; consequently, the critical exponents obtained by MQMC are reasonably consistent with RG calculations.

Other sign-free models in MQMC. We have shown that MQMC, as an auxiliary field QMC approach, can solve the fermion sign problem in a class of *spinless* fermion models by utilizing the Majorana representation of complex fermions. It will be straightforward to generalize the current MQMC algorithm to solve the fermion sign problem in interacting fermion models with more than one fermion species. Such MQMC fermion-sign-free models include the $SU(N = \text{odd})$ negative-U Hubbard model on bipartite lattices whose Hamiltonian is given by

$$H = -t \sum_{\langle ij \rangle} \left[\sum_{\alpha=1}^{N} c_{i\alpha}^\dagger c_{j\alpha} + \mathrm{H.c.} \right] + U \sum_i \left[n_i - \frac{N}{2} \right]^2, \quad (22)$$

where $U < 0$. This model on the honeycomb lattice has a similar semimetal to CDW transition even though the quantum critical exponents can depend on N.

More importantly, we can show that the following $SU(N = \text{odd})$ fermionic model,

$$H = -t \sum_{\langle ij \rangle} \left[\sum_{\alpha=1}^{N} c_{i\alpha}^\dagger c_{j\alpha} + \mathrm{H.c.} \right] - J \sum_{\langle ij \rangle} [c_{i\alpha}^\dagger c_{j\alpha} + \mathrm{H.c.}]^2, \quad (23)$$

is sign free in MQMC when the lattice is bipartite and $J > 0$. It is worth stressing that this class of $SU(N)$ models is sign free

only in the MQMC method but encounters the sign problem in other QMC methods, such as CTQMC [20,22]. This shows that the MQMC algorithm discovered by us can solve the fermion sign of models which go beyond those solvable by CTQMC and other conventional QMC methods.

We thank Fakher Assaad, Alexei Kitaev, Ziyang Meng, and Lei Wang for helpful discussions. This work is supported in part by the National Thousand-Young-Talents Program (H.Y.) and by the NSFC under Grant No. 11474175 (Z.X.L., Y.F.J., and H.Y.).

[1] X.-G. Wen, *Quantum Field Theory of Many-Body Systems* (Oxford University Press, New York, 2004).
[2] E. Fradkin, *Field Theories of Condensed Matter Physics*, 2nd ed. (Cambridge University Press, Cambridge, U.K., 2013).
[3] D. J. Scalapino and R. L. Sugar, Phys. Rev. Lett. **46**, 519 (1981).
[4] R. Blankenbecler, D. J. Scalapino, and R. L. Sugar, Phys. Rev. D **24**, 2278 (1981).
[5] F. Fucito, E. Marinari, G. Parisi, and C. Rebbi, Nucl. Phys. B **180**, 369 (1981).
[6] J. E. Hirsch, D. J. Scalapino, R. L. Sugar, and R. Blankenbecler, Phys. Rev. Lett. **47**, 1628 (1981).
[7] J. E. Hirsch, Phys. Rev. B **31**, 4403 (1985).
[8] E. Y. Loh, J. E. Gubernatis, R. T. Scalettar, S. R. White, D. J. Scalapino, and R. L. Sugar, Phys. Rev. B **41**, 9301 (1990).
[9] M. Troyer and U.-J. Wiese, Phys. Rev. Lett. **94**, 170201 (2005).
[10] A negative sign in quantum magnets with frustrated superexchange interactions is also a consequence of the fermionic minus sign of the superexchange process.
[11] J. E. Hirsch and R. M. Fye, Phys. Rev. Lett. **56**, 2521 (1986).
[12] S. Hands, I. Montvay, S. Morrison, M. Oevers, L. Scorzato, and J. Skullerud, Eur. Phys. J. C **17**, 285 (2000).
[13] C. Wu and S.-C. Zhang, Phys. Rev. B **71**, 155115 (2005).
[14] E. Berg, M. A. Metlitski, and S. Sachdev, Science **338**, 1606 (2012).
[15] M. Hohenadler, Z. Y. Meng, T. C. Lang, S. Wessel, A. Muramatsu, and F. F. Assaad, Phys. Rev. B **85**, 115132 (2012).
[16] D. Zheng, G.-M. Zhang, and C. Wu, Phys. Rev. B **84**, 205121 (2011).
[17] W. Bietenholz, A. Pochinsky, and U.-J. Wiese, Phys. Rev. Lett. **75**, 4524 (1995).
[18] S. Chandrasekharan and U.-J. Wiese, Phys. Rev. Lett. **83**, 3116 (1999).
[19] S. Chandrasekharan, Eur. Phys. J. A **49**, 90 (2013).
[20] E. F. Huffman and S. Chandrasekharan, Phys. Rev. B **89**, 111101 (2014).
[21] E. Gull, A. J. Millis, A. I. Lichtenstein, A. N. Rubtsov, M. Troyer, and P. Werner, Rev. Mod. Phys. **83**, 349 (2011).
[22] L. Wang, P. Corboz, and M. Troyer, New J. Phys. **16**, 103008 (2014).
[23] L. Wang and M. Troyer, Phys. Rev. Lett. **113**, 110401 (2014).
[24] A more efficient continuous-time QMC algorithm was introduced recently. See M. Iazzi and M. Troyer, Phys. Rev. B **91**, 241118 (2015); L. Wang, M. Iazzi, P. Corboz, and M. Troyer, *ibid.* **91**, 235151 (2015).
[25] Z.-X. Li, Y.-F. Jiang, and H. Yao, arXiv:1411.7383, New J. Phys. (to be published).
[26] S. Raghu, X.-L. Qi, C. Honerkamp, and S.-C. Zhang, Phys. Rev. Lett. **100**, 156401 (2008).
[27] S.-K. Jian, Y.-F. Jiang, and H. Yao, Phys. Rev. Lett. **114**, 237001 (2015).
[28] See Supplemental Material at http://link.aps.org/supplemental/10.1103/PhysRevB.91.241117 for details.
[29] G. Sugiyama and S. Koogin, Ann. Phys. **168**, 1 (1986).
[30] S. Sorella, S. Baroni, R. Car, and M. Parrinello, Europhys. Lett. **8**, 663 (1989).
[31] S. R. White, D. J. Scalapino, R. L. Sugar, E. Y. Loh, J. E. Gubernatis, and R. T. Scalettar, Phys. Rev. B **40**, 506 (1989).
[32] P. Calabrese and J. Cardy, J. Stat. Mech.: Theory Exp. (2004) P06002.
[33] A. Kitaev and J. Preskill, Phys. Rev. Lett. **96**, 110404 (2006).
[34] M. Levin and X.-G. Wen, Phys. Rev. Lett. **96**, 110405 (2006).
[35] H. Li and F. D. M. Haldane, Phys. Rev. Lett. **101**, 010504 (2008).
[36] J. Eisert, M. Cramer, and M. B. Plenio, Rev. Mod. Phys. **82**, 277 (2010).
[37] T. Grover, Phys. Rev. Lett. **111**, 130402 (2013).
[38] F. F. Assaad, T. C. Lang, and F. Parisen Toldin, Phys. Rev. B **89**, 125121 (2014).
[39] S. Sachdev, *Quantum Phase Transitions*, 2nd ed. (Cambridge University Press, Cambridge, U.K., 2011).
[40] L. Janssen and I. F. Herbut, Phys. Rev. B **89**, 205403 (2014).